2021 Joint European Conference on Networks and Communications & 6G Summit (EuCNC/6G Summit) | 978-1-6654-1526-2/21/$31.00 ©2021 IEEE | DOI: 10.1109/EUCNC/6GSUMMIT51104.2021.9482525

Evaluating a Novel Bluetooth 5.1 AoA Approach for Low-Cost Indoor Vehicle Tracking via Simulation

Nuno Paulino and Luís M. Pessoa
INESC TEC and Faculty of Engineering,
University of Porto, Porto, PORTUGAL
{nuno.m.paulino, luis.m.pessoa}@inesctec.pt

André Branquinho and Edgar Gonçalves
Wavecom – Soluções Rádio SA,
Aveiro, PORTUGAL
{abranquinho, egoncalves}@wavecom.pt

***Abstract*—The recent Bluetooth 5.1 specification introduced the use of Angle-of-Arrival (AoA) information which enables the design of novel low-cost indoor positioning systems. Existing approaches rely on multiple fixed gateways equipped with antenna arrays, in order to determine the location of an arbitrary number of simple mobile omni-directional emitters. In this paper, we instead present an approach where mobile receivers are equipped with antenna arrays, and the fixed infrastructure is composed of battery-powered beacons. We implement a simulator to evaluate the solution using a real-world data set of AoA measurements. We evaluated the solution as a function of the number of beacons, their transmission period, and algorithmic parameters of the position estimation. Sub-meter accuracy is achievable using 1 beacon per $15\,\mathrm{m}^2$ and a beacon transmission period of $500\,\mathrm{ms}$.**

I. Introduction

With the trend towards edge computing and the Internet-of-Things (IoT), there is an increased need for smarter devices capable of operating with greater autonomy from conventional centralized systems. One application in this domain is the indoor localization and tracking of assets [1]. While outdoor tracking is possible in real-time and with great accuracy, indoor environments still lack a standard solution that is accurate and scalable. The Bluetooth 5.1 specification introduced new opportunities for low-cost indoor localisation through the use of AoA of transmissions. Computing the AoA of a received packet requires the receiver to be equipped with an antenna array. The Bluetooth 5.1 specification defines that a packet for direction finding is terminated with a Constant Tone Extension (CTE) of configurable length [2]. The receiver samples its antennas during this period, and by determining the difference in carrier phase between pairs of antennas, the angle of the incident plane wave front can be estimated [1].

Relative to AoA, other techniques for indoor localisation present significant disadvantages. For example, the localisation of a receiver relative to several transmitters can be estimated based on signal Received Signal Strength Indications (RSSIs). However, the RSSI is unpredictably subject to noise, or the relative orientation of the antennas. Other techniques include Time-Difference-of-Arrival (TDoA), where a mobile receiver computes the difference between arrival times of packets from fixed transmitters. However, a very precise synchronization is required between transmitters. For example, Ultra-Wide-Band (UWB) based solutions rely on TDoA. Although high accuracy is possible (under $10\,\mathrm{cm}$), UWB systems require precise synchronization between the fixed receiving anchors, meaning dedicated cable installations are required on-site. In contrast, the AoA does not vary based on RSSI and functions for an arbitrary number of non-synchronized transmitters, and can be easily installed in existing locations. The technology is also used in WiFi gateways, but in conjunction with Bluetooth, future solutions promise scalability and low-cost.

Conventional AoA localisation is based on fixed wall-powered receivers with antenna arrays, which receive pings from mobile emitters (e.g., smartphones). The AoA data is transmitted to a centralized server, which estimates transmitter positions and returns this information to them, e.g., via WiFi. This solution is suited for scenarios with an arbitrarily large number of ubiquitous simple transmitters (such as crowds in shopping malls or exhibition halls). However it imposes a higher infrastructure cost to ensure good coverage and localisation accuracy, due to costly wall-powered gateways with antenna arrays.

Instead, we propose a network topology consisting of a potentially large number of fixed Bluetooth Low Energy (BLE) battery-powered beacons with omni-directional antennas. Mobile receivers with antenna arrays can then exploit this low-cost infrastructure to estimate their own position. By accumulating received packets and using a known table of absolute beacon positions, each receiver can autonomously locate itself on a known map, without the need for a centralized infrastructure. Compared to fixed receivers with antenna arrays, our approach is more scalable, as low-cost beacons can be deployed flexibly in existing locations (e.g., factories and warehouses) without an existing power supply infrastructure. Our main application scenario is the self-localization of forklifts and similar vehicles in warehouses or similar industrial locations.

We provide a brief analysis of the state-of-the-art in Section II, and present our approach in Section III. In Section IV we detail how we implement a simulation of the solution, and in Section V we provide the respective experimental evaluation. We demonstrate expected localisation and tracking performance as a function of solution parameters such as the number of beacons, their transmission period, and position estimation parameters. In Section VI we conclude the paper. By implementing the AoA calculation algorithms for the proposed topology in a configurable simulator, which relies on real-world AoA data, we demonstrate that sub-meter accuracy can be achieved for a receiver traveling at $10\,\mathrm{km\,h^{-1}}$, using 1 beacon per $15\,\mathrm{m}$, transmitting at $500\,\mathrm{ms}$.

Authorized licensed use limited to: b-on: UNIVERSIDADE DO PORTO. Downloaded on May 05,2023 at 09:23:24 UTC from IEEE Xplore. Restrictions apply.

II. Related Work

Past Bluetooth based solutions rely on RSSI, achieving location accuracy between 20 cm to 3 m [3]–[6]. The best results are achieved by resorting to fingerprinting of the location area. In [6], a density of 1 beacon per 25 m achieves sub-meter accuracy with a beacon transmission period of 100 ms, but the results are subject to the fingerprinting of the location becoming outdated, or to interference with other devices. For the same transmission period, we achieve sub-meter accuracy with a comparable density of 1 beacon per 22 m. Unlike fingerprinting methods, AoA based localisation does not require learning the characteristics of the environment, and can easily adapt to changing beacon positions, or faulty beacons, given enough redundancy.

In [5] the quality of the AoA samples is improved using the Multiple Signal Classification (MUSIC) algorithm. Two fixed anchors are used, each with 4 dipole antennas in a linear configuration. An average accuracy of 14 cm is achieved when locating the stationary beacon, for the 36 test positions.

In [7] a scenario with fixed receivers with 2 antennas is evaluated. Software-defined radios emulate the specification of packets with CTE. Each receiver is equipped with two half-wavelength dipole antennas. The approach computes the localisation of a single beacon, based on the AoA of received packets, and the receiver's known absolute positions. The accuracy of the AoA measurements is evaluated for a range of 15°–90° in steps of 5°, obtaining standard deviations from the true angle between 0.2° and 2°. A detailed analysis is given on the relationship between measurement error, value of the true angle, and the specific data channels and carrier frequency employed. The position estimation error is below 0.85 m for 95 % of the true positions tested.

The use of data fusion methods and several filtering steps, including a Kalman filter and a curve fitting step, are studied in [8] to improve AoA sample quality. The Kalman filter is applied to reduce errors between several values of the phase difference between the same antenna pair. A Gaussian filter is applied to compensate for AoA errors which vary according to the channel used for transmission. To configure the filter, the authors experimentally evaluated the error AoA induced by each channel. To evaluate the approach, two transmitters and one receiver are used. The receiver contains two arrays with 3 elements each, resulting in contiguous AoA measurement range of $-180°$ to $180°$. Significant accuracy improvements are achieved for a true angle range of $-60°$ to $60°$.

III. Proposed Approach

Existing approaches for mobile device self-localization target scenarios with an arbitrary number of devices (e.g., cellphones) relying on a centralized localization server, and on a mesh of fixed wall-powered receivers with antenna arrays. Given our scenario of warehouse vehicle location, where the number of mobile receivers is fewer, we propose to instead equip these with antenna arrays, to use cheaper battery powered beacons, and to remove the need for the centralized infrastructure. In this section we detail the AoA based position estimation methods, the real-world data set we employed in experimental evaluation, and our formulation for receiver trajectory tracking.

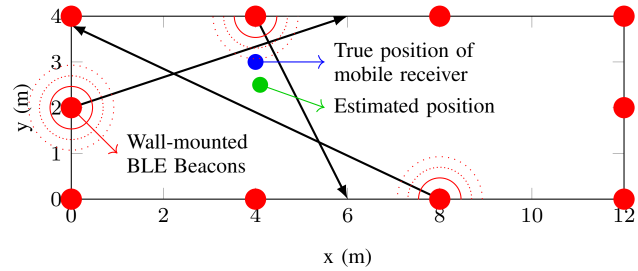

Fig. 1. Estimation of position via received AoA and least-squares method, for 3 wall-mounted BLE beacons in a short 12x4 m corridor. Angle measurements are affected by errors, which create a candidate area.

A. Position Estimation via Least Squares

Estimation of position from received angles is based on the assumption that the receiver knows the absolute position of each transmitter, and that each received packet is annotated with a beacon identifier. In an ideal scenario, two direction vectors derived from two beacons originating from different transmitters would be sufficient to compute a single point corresponding to the receiver location. However, due to errors in the measured angle (i.e., from reflections or measurement errors), a greater number of direction vectors are required. Even so, regardless of the number of direction vectors, there will be no single intersection point due to errors. An example is illustrated in Figure 1, where AoA measurement errors from three wall mounted beacons leads to a candidate area.

To estimate a position, we resort to a state-of-the-art least-squares method which computes the point which minimizes the total distance to all lines [9], [10]. The respective formulation is summarized in Equations (1) to (3).

$$n_j = [x_j, y_j]^\top, \quad \|n_j\| = 1 \tag{1}$$

$$R = \sum_{j=1}^{K} c_j(I - n_j n_j^\top), \quad q = \sum_{j=1}^{K} c_j(I - n_j n_j^\top)a_j \tag{2}$$

$$R \cdot p = q \tag{3}$$

Where c_j represents the confidence level (i.e., weight) in angle measurement j, and a_j represents the known position of the respective beacon. For each measurement, a normalized vector n_j with origin at a_j is computed. Matrices R and q compose a system of equations derived from a deduction of a point p which minimizes the sum of distances of p to each line. We resort to an available implementation of a linear solver to compute p from known matrices R and q [11].

B. Real-World Data

In order to achieve more realistic simulation, the angle used in position estimation was sampled from a real-world data set we constructed experimentally. We used a commercial Telink TLSR8258 antenna array board with 8 antennas, mounted on a rotating support with controllable angle. We placed a BLE transmitter and the receiver at a distance of 4.3 m, in a non-ideal (cluttered) room of approximately 10 m by 7 m. We completed a full rotation of the receiver, in steps of 10°, and for every step we collected 1000 samples of the measured angle [12]. Figure 2 shows the resulting distribution of measured angles as 36 box plots, plotted versus the true angle. Although

Authorized licensed use limited to: b-on: UNIVERSIDADE DO PORTO. Downloaded on May 05,2023 at 09:23:24 UTC from IEEE Xplore. Restrictions apply.

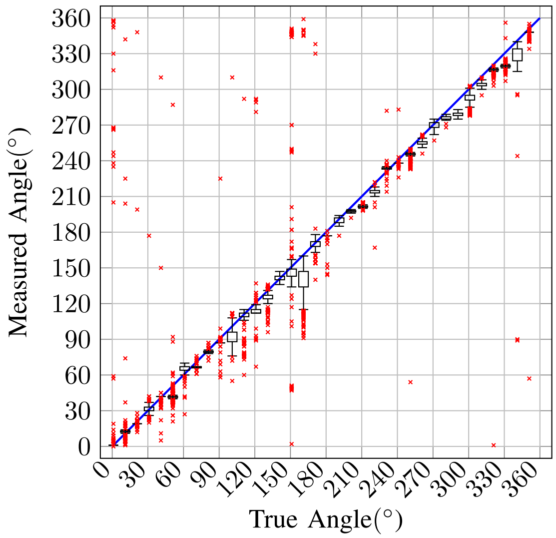

Fig. 2. True angles vs. respective 1000 samples of measured angle for a Telink TLSR8258 8-Antenna board in an uncontrolled indoor environment

the mean of each boxplot is within a $4\,\%$ error of the true angle, there are significant outliers for arbitrary true angle values, which are likely due to reflections. Since it is impossible to disambiguate an erroneous measurement (i.e., outlier) from a reliable one (e.g., measuring an angle of $270°$ for a true angle of $150°$), we implemented a pre-processing step which filters likely outliers. This is explained in Section V.

During simulation, the true angle of the receiver to each transmitter is known to the simulator. To estimate a measured angle, we sample one of the thousand data points of the nearest available angle (e.g., for a true angle of $3°$ we sample real world measurements from $0°$). Additionally, the average error for any true angle is non-zero. For any true angle, the average error is approximately $-5°$. Knowing this characteristic of the receiver, we apply a correction to this measurement offset during simulation when estimating a measured angle.

C. Kalman Filter

In order to track the movement of the receiver, we employ a first-order Kalman Filter [13]. The state vector $\hat{x}$ represents the position and velocity of the receiver in two-dimensional space. The following are the matrices which define the filter's operation, according to its canonical formulation.

$$x = \begin{bmatrix} x_\mathrm{x} \\ x_\mathrm{y} \\ \dot{x}_\mathrm{x} \\ \dot{x}_\mathrm{y} \end{bmatrix} \quad F = \begin{bmatrix} 1 & 0 & dt & 0 \\ 0 & 1 & 0 & dt \\ 0 & 0 & 1 & 0 \\ 0 & 0 & 0 & 1 \end{bmatrix} \quad H = I(4) \quad P = I(4) \cdot \sigma_s \tag{4}$$

$$R = \begin{bmatrix} \sigma_s & 0 & 0 & 0 \\ 0 & \sigma_s & 0 & 0 \\ 0 & 0 & 1 & 0 \\ 0 & 0 & 0 & 1 \end{bmatrix} \quad Q = \begin{bmatrix} \frac{dt^4}{4} & 0 & \frac{dt^3}{2} & 0 \\ 0 & \frac{dt^4}{4} & 0 & \frac{dt^3}{2} \\ dt^3 & 0 & dt^2 & 0 \\ 0 & dt^3 & 0 & dt^2 \end{bmatrix} \cdot \sigma_{\hat{x}}^2 \tag{5}$$

The value dt represents the filter time-step, i.e., the period at which the filter is evaluated. The receiver can describe arbitrary trajectories in the two-dimensional space, with independent behaviour in each orthogonal axis. Therefore, there are no co-variance components between x and y in the R and Q matrices. The values of σ_s and $\sigma_{\hat{x}}$ represent the expected standard deviation of the measurement noise, and the process noise (i.e., uncertainty), respectively. The former relates to the accuracy of position estimation based on AoA, while the latter is intrinsic to the receiver movement. Low values for $\sigma_{\hat{x}}$ represent higher confidence in the position samples given to the filter, while higher values represent higher confidence in the filter predictions. For completeness, the canonical *predict* – Equation (6) – and *update* – Equations (7) and (8) – steps of the Kalman filter used are given as follows:

$$\hat{x} = F\hat{x}, \quad P = FPF^\top + Q \tag{6}$$

$$y = [p_\mathrm{x}, p_\mathrm{y}, \dot{p_\mathrm{x}}, \dot{p_\mathrm{y}}]^\top, \quad I = y - H\hat{x} \tag{7}$$

$$S = HPH^\top + R, \quad K = PHS^{-1}, \quad \hat{x} = \hat{x} + KI \tag{8}$$

Where column matrix y represents a new sample of position estimation computed via the AoA geometry described previously, and the respective estimated velocity based on previous position data.

IV. Simulation

In order to evaluate the solution, we developed a Java based simulator which implements the algorithms described in previous sections. The simulator models a two-dimensional map of configurable width and height, which contains a specified number of *beacon* objects and a single mobile *receiver* object. The simulator does not model physical effects such as reflections, RSSI, the transmitter/receiver radios, or the Bluetooth software stack. It's primary purpose is to evaluate the tracking accuracy for the solution topology based on real-angle measurement data, and as a function of other parameters of the solution (e.g., number of beacons or Kalman filter tuning). Table I lists the major parameters of the simulation which can be adjusted. Where a constant value is indicated, the respective parameter was set at that value for all experimental evaluations. Where value ranges are indicated, this represents the sweeps performed in Section V to evaluate the performance as a function of the respective parameter.

A. Functional Description

The simulator evaluates the map state in time steps of $1\,\mathrm{ms}$. The map may contain any number of beacon objects at any position, and one mobile receiver which follows a trajectory described by a parametric function. At every time-step, events generated by the *beacons* and *receiver* are evaluated. Simulation ends after a specified time interval. Since in real-world conditions, separate devices would not be accurately synchronized, each object contains its own internal timer and triggers its periodic events (e.g., packet transmission) based on its value.

a) Beacons: The only event triggered by each beacon is the generation of a packet at a given period. Packets are placed into a self-evicting queue, and are sampled by the receiver in order of insertion. Packets are only placed into the queue if the respective beacon is located less than $20\,\mathrm{m}$ from the receiver, which is a simplified emulation of transmission range. Also, the desynchronized event timers create a more realistic behaviour where, despite the same b_p for all transmitters, packets are received at arbitrary intervals by the receiver. Additionally, they ensure that the b_c instantiated beacons do not saturate the queue which represents the air medium, by simultaneously creating packets at the same time-step. For clarity, the simulator does not implement electromagnetic events such as contention for the transmission medium.

Authorized licensed use limited to: b-on: UNIVERSIDADE DO PORTO. Downloaded on May 05,2023 at 09:23:24 UTC from IEEE Xplore. Restrictions apply.

TABLE I. CONFIGURABLE SIMULATION PARAMETERS

Parameter	Description	Value(s)
R_x, R_y	Map dimensions	100x4 m
b_p	Packet generation period of beacons	100 ms–1000 ms
b_c	Number of beacons on the map	4–64
σ_s	Estimated noise of measurements ($\hat{p}$)	1 m
$\sigma_{\hat{x}}$	Estimated noise of movement process	0 m–3 m
K_p	Time step of *predict* step	2 ms
K_u	Time step of *update* step	$K_u(b_c, b_p, p_c)$
p_c	Number of packets used in LSQ method	3–50
Trajectory	Parametric functions $x = f(t)$, $y = g(t)$	Sinusoidal path
Weight Policy	Policy for computing weights c_j of LSQ	(W_u, W_r, W_t)

b) Receiver: The receiver contains a list of events that are evaluated at different periods. The movement is updated at every time-step (i.e., 1 ms), as well as the sampling of the packet queue. The Kalman *predict* step is performed every $dt = 2\,\mathrm{ms}$, while the Kalman *update* step is performed at a non-constant step. Since a position can only be estimated based on available data (i.e., sufficient packets), the *update* step is aperiodic. Additionally, the measurement vector y also contains the estimated velocity. We compute it as the difference between the last receiver position produced by the Kalman filter and the new position estimate p. An estimate is only computed if a sufficient number of packets have been read by the receiver from the queue. This number of packets used is configurable, and its effects are shown in Section V. Once p is computed, the receiver discards its held packets. That is, packets are not re-used for successive estimates of p. Finally, although the position of the receiver is modeled, we do not model its orientation. Calculations assume that the receiver is facing an orientation given by vector $v = [1, 0]$ at all times.

c) Packet Filtering: In order to discard erroneous AoA measurements, we attempted to accumulate multiple packets per beacon prior to computing a position estimation. By computing the median of all samples for each beacon, we then discard any samples which differed from the median by more than 2°. We compared this policy to utilizing all available packets, by varying other simulation parameters for both cases.

d) RSSI Estimation: We evaluated the use of RSSI to attribute weights to each received packet, for the posterior step of LSQ estimation. We do this by evaluating the Friis transmission equation using the true (hidden) distance between the receiver. We assume a transmission power of 0 dBm.

e) Computing weights c_j for LSQ Estimation: We evaluated three policies for packets weights. The first attributes a weight of 1 for all samples (W_u). The second and third perform a linear normalization between a maximum weight of 1 and a minimum of 0.8, according to Equation (9).

$$c_j = 1 + \left(\frac{0.2}{max_v - min_v}\right)(v_j - max_v) \tag{9}$$

Where values max_v, min_v, and v_j depend on policy. For policy W_r, the first two values represent the maximum and minimum RSSI for all samples, and the third represents the value for sample j (i.e., lower weight is given to distant beacons). For policy W_t, they represent the analogous values for the reception times of the samples (i.e., lower weight is given to older accumulated samples).

V. EXPERIMENTAL RESULTS

We evaluate the proposed solution using the simulation environment described above. Our objective was to determine if sub-meter localisation accuracy based on BLE AoA is feasible. Specifically, we wished to determine the minimum number of beacons required, and to minimize their transmission period, as these are the two factors which determine the cost of the solution. For all experimental evaluations and parameter sweeps, we configured the simulator such that the receiver travels in a sinusoidal trajectory at $10\,\mathrm{km\,h^{-1}}$ in a $100\,\mathrm{m}$ long corridor of $4\,\mathrm{m}$ in width. Unless stated otherwise, other parameters are: $\sigma_s = 1.0$, no packet filtering, the packet weight policy is W_u, and the number of packets used for position estimation is $p_c = 6$. The AoA was sampled from the real-world data set described in Section III-B. We evaluated the quality of the solution by computing the Root mean square error (RMSE) between the true trajectory, and the output trajectory of the Kalman Filter. In the following sections we tune the solution parameters based on the attainable RMSE.

A. Parameter Tuning

The solution is composed of a number of interdependent parameters. As such, an iterative tuning process was required. For brevity, we will present the attainable RMSE as a function of sweeps of multiple parameters. For each sweep, other parameters are held constant at specified values. Firstly, we determine the best value for $\sigma_{\hat{x}}$, under the stipulated simulation conditions. Secondly, we determine the number of packets to use that results in the best position estimations via the proposed LSQ method. Thirdly, we evaluate the RMSE as a function of both b_p and b_c. Finally, we demonstrate examples of the produced trajectories, computed positions estimations, and Kalman filter output.

a) Determining $\sigma_{\hat{x}}$: Figure 3 illustrates the RMSE obtainable as a function of the $\sigma_{\hat{x}}$ parameter of the Kalman filter, for three values of b_p. We set the b_c at 128 to prevent bad performance due to lack of beacons. Although the behaviour for greater values of b_p diverges for values of $\sigma_{\hat{x}}$ significantly greater than 1 m, we observe that there is a minimum for approximately $0.32\,\mathrm{m}$. With greater values for $\sigma_{\hat{x}}$, the tracked position tends to match the estimated positions, which are noisy, leading to greater RMSE. For very low values, the filter has as slower response. For other movement speeds, the best $\sigma_{\hat{x}}$ is likely to change, but we can observe sub-meter accuracy for the evaluated range, for multiple values of b_p. The RMSE for greater b_p values increases more quickly for $\sigma_{\hat{x}} > 0.5$, since samples are available less readily. The filter thus estimates the receiver velocity based on sparse noisy samples. However, the minimum at $\sigma_{\hat{x}} \approx 0.32$ holds for values of b_p up to $1000\,\mathrm{ms}$.

b) Effect of Packet Count (p_c): Each position estimation is performed when p_c packets are available. Figure 4 shows how the RMSE varies according to this parameter, for 6 combinations of b_p and b_c. Neither of these two parameters influences the value of p_c which minimizes the RMSE. For greater values of p_c the receiver travels a greater distance until enough packets are accumulated (which varies as a function of b_p and b_c). This leads to greater likelihood of more samples for any one beacon, and more spatial diversity in the beacon sampling. However, the samples now correspond to different

Authorized licensed use limited to: b-on: UNIVERSIDADE DO PORTO. Downloaded on May 05,2023 at 09:23:24 UTC from IEEE Xplore. Restrictions apply.

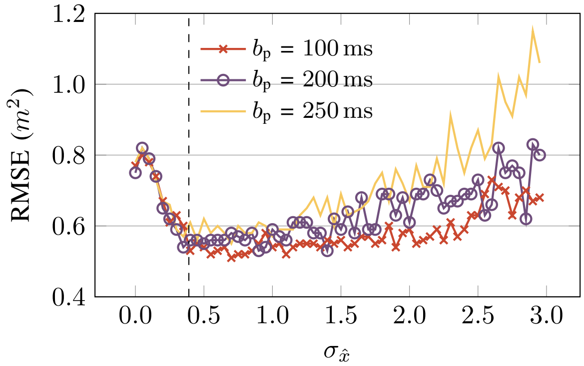

Fig. 3. Root Mean Square Error as a function of $\sigma_{\hat{x}}$ for different beacon periods, b_p, for the total sinusoidal trajectory ($b_c = 64$, $p_c = 6$).

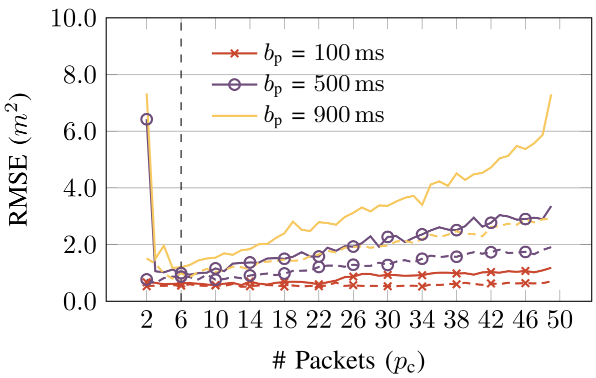

Fig. 4. Root Mean Square Error as a function of the number of packets (p_c) used for position estimation, for different beacon periods (b_p) and beacon counts (b_c). Solid lines represent $b_c = 32$ and dashed lines represent $b_c = 64$.

true positions, which leads to poorer performance. Noticeably, for $(b_c, b_p) = (64, 100)$ the performance remains near constant for any value of p_c. Since beacons are densely placed, and the period is low, packets corresponding to the same true position can be gathered before any significant receiver movement. However, the solution does no improve past $p_c = 6$ as the AoA information becomes redundant. Although 6 packets are used to estimate each position for other results shown in this section, we did not analyse their spatial distribution. However, since the beacons are homogeneously distributed, and transmit at the same period, it is expectable that random samples of 6 beacons within the receiver range would yield a respectively homogeneous spatial distribution (i.e., it is unlikely that a batch of 6 packets originated from physically proximate beacons).

c) Effect of Beacon Count (b_c) and Beacon Period (b_p): The number of beacons and their transmission period have the most significant effect on the RMSE, as expected. Since we desire frequent position estimation for tracking, solutions with either high b_p or low b_c, or both, lead to poorer results. Figure 5 shows the performance for a range of b_c values and three b_p values. Several solutions provide sub-meter accuracy, e.g., $(b_c, b_p) = (16, 100)$ or $(b_c, b_p) = (64, 900)$. Since beacons are placed along the map perimeter, the former solution corresponds to placing one beacon every 12.5 m, and the later to placing one beacon every 3.2 m. Both solutions provide similar RMSE ($\approx 1m^2$), but the case for $(b_c, b_p) = (64, 900)$

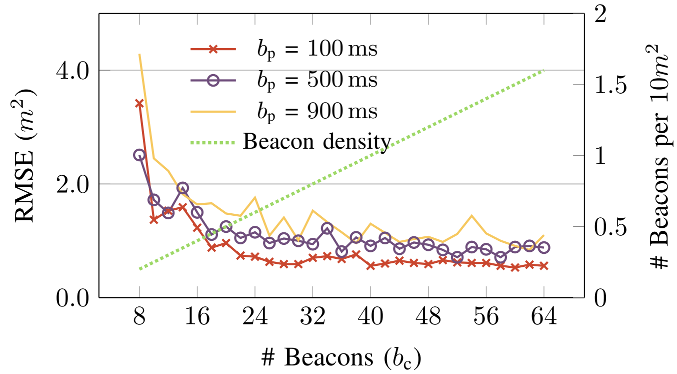

Fig. 5. Root Mean Square Error as a function of the number of beacons (b_c), for different beacon periods (b_p), and number of beacons per $10\,\mathrm{m}^2$ (assuming the area of the simulated 100x4 m room).

allows for a $9\times$ decrease in beacon activity, and therefore a potential for equivalent battery savings, despite requiring only a $4\times$ higher b_c relative to the case for $(b_c, b_p) = (16, 100)$. Conversely, although the RMSE for $b_p = 100$ is approximately half than that for $b_p = 900$ when $b_c = 64$, $9\times$ higher beacon activity is required. The more cost effective solution will depend on actual one-time infrastructure costs and battery maintenance costs. This analysis is out of the scope of this evaluation.

d) Effect of Packet Weight and Filtering Policies: We performed the parameter sweeps shown in Figures 3 to 5, for combinations of the filtering and weight policies, but omit the respective plots for brevity. Summarily, we observed no improvements over no filtering and policy W_u. In order for both filtering and weighting to induce any actual effect, larger batches of samples are required. For filtering, more than 5 samples per beacon are required. However, when p_c is low (e.g. 6), position estimation will proceed with very few samples per beacon. As a result, filtering has no effect, and the weights applied by linear regression reduce the contribution of samples which are either temporally close (W_t) or of similar RSSI (W_r). The complete interaction is difficult to evaluate given the interdependence between p_c and the rate at which packets are received, which is a function of b_p and b_c.

B. *Trajectory Tracking Examples*

Previous sections demonstrated the effect of several parameters on the RMSE of a complete sinusoidal trajectory. Figure 6 illustrates the full trajectory in top-down view of the two dimensional map. Note that the axes are not normalized. Beacons are not plotted, but are evenly spaced along the map perimeter for all cases. Figure 6a shows the tracking performance as a function of b_c, for $b_p = 500$, and Figure 6b shows the tracking as a function of b_p, for $b_c = 64$. Since the simulation is subject to randomness, we repeated each shown run with the same values of (b_c, b_p) (and other parameters) 100 times to obtain a noise free RMSE. For $(b_c, b_p) = (64, 500)$, $(b_c, b_p) = (32, 500)$, $(b_c, b_p) = (16, 500)$, the RMSE is $0.77\,\mathrm{m}^2$, $0.98\,\mathrm{m}^2$, $1.4\,\mathrm{m}^2$, respectively. For $(b_c, b_p) = (64, 100)$, $(b_c, b_p) = (64, 500)$, $(b_c, b_p) = (64, 1000)$, the RMSE is $0.53\,\mathrm{m}^2$, $0.76\,\mathrm{m}^2$, $1.07\,\mathrm{m}^2$, respectively. These values are consistent with Figure 5.

Authorized licensed use limited to: b-on: UNIVERSIDADE DO PORTO. Downloaded on May 05,2023 at 09:23:24 UTC from IEEE Xplore. Restrictions apply.

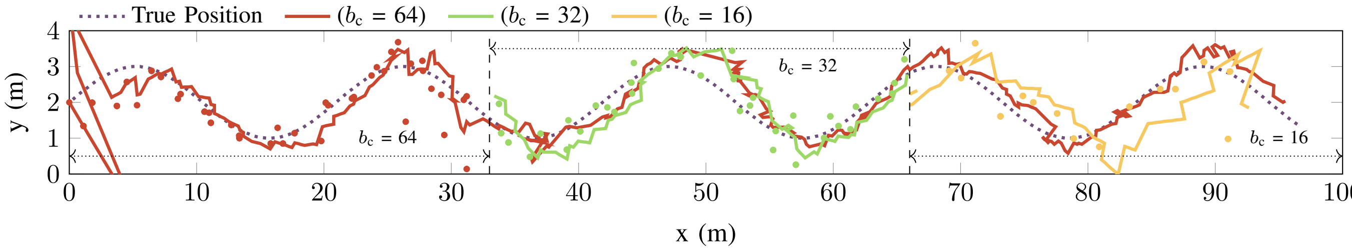

(a) Travelled sinusoidal trajectory and filter output for 64, 32, and 16 beacons ($\sigma_s = 1.0$, $\sigma_{\hat{x}} = 0.32$, $b_p = 500ms$, $p_c = 6$).

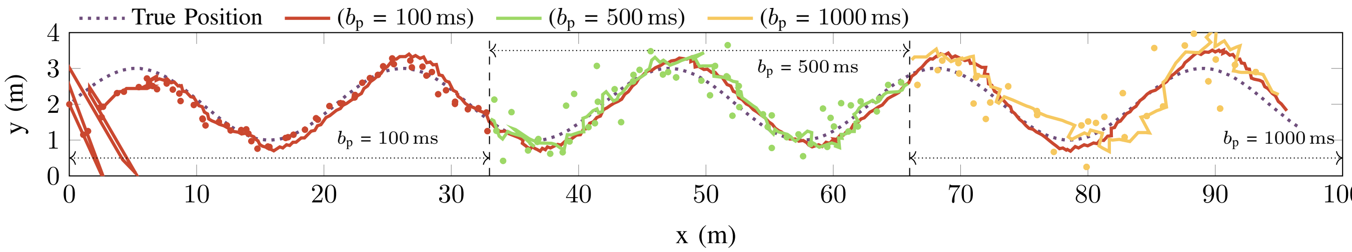

(b) Travelled sinusoidal trajectory and filter output for $b_c = 64$ beacons, for several beacon periods ($\sigma_s = 1.0$, $\sigma_{\hat{x}} = 0.32$, $b_c = 64$, $p_c = 6$).

Fig. 6. Tracked trajectories for values of b_p and b_c. Full trajectories are shown for $(b_c, b_p) = (64, 500)$ (Figure 6a) and for $(b_c, b_p) = (64, 100)$ (Figure 6b). For clarity, other trajectories are shown partially, and the estimated positions fed to the Kalman filter are plotted accordingly. As b_c decreases, and/or b_p increases, the receiver travels a longer period before accumulating $p_c = 6$ sample which correspond to different true positions, leading to sparser and noisier samples.

VI. Conclusion

In this paper, we presented an evaluation of a BLE topology for indoor asset localisation and tracking, based on AoA capabilities of the Bluetooth 5.1 specification. Specifically, the approach targets the use case of few mobile receivers which require their own localisation in real-time. The solution aims to reduce costs, by designing the fixed infrastructure as battery powered omni-directional beacons. We developed a simulator which implemented the proposed topology, position estimation, and tracking methods. We evaluated the RMSE of the tracked trajectory versus the true trajectory, along a $100\text{x}4\,\text{m}$ corridor, for multiple number of beacons, beacon periods, Kalman filter parameters, and heuristic policies. We predict, based on the modeling of the proposed solution, and on real-world angle measurements taken in non-ideal environments, that localisation accuracy under $1\,\text{m}$ can be achieved for a beacon period of $500\,\text{ms}$ and beacon placements every $3.2\,\text{m}$ along the corridor walls. Future work will include the modeling of reflections and obstructions, gather additional real-world AoA data, and other heuristics for handling received packets to improve the achievable RMSE for arbitrary trajectories.

Acknowledgment

This work is financed by the ERDF – European Regional Development Fund through the Operational Programme for Competitiveness and Internationalisation - COMPETE 2020 Programme within project SLID: Stock Live IDentification (POCI-01-0247-FEDER-045388).

References

[1] F. Zafari, A. Gkelias, and K. K. Leung, "A Survey of Indoor Localization Systems and Technologies," *IEEE Communications Surveys Tutorials*, vol. 21, no. 3, pp. 2568–2599, 2019.

[2] Bluetooth SIG, "Bluetooth Specification Version 5.1," 2019. [Online]. Available: https://www.bluetooth.com/wp-content/uploads/2019/03/1901_Feature_Overview_Brief_FINAL.pdf

[3] R. Faragher and R. Harle, "Location Fingerprinting With Bluetooth Low Energy Beacons," *IEEE Journal on Selected Areas in Communications*, vol. 33, no. 11, pp. 2418–2428, 2015.

[4] X. Zhao, Z. Xiao, A. Markham, N. Trigoni, and Y. Ren, "Does BTLE measure up against WiFi? A comparison of indoor location performance," in *In Proc. of the 20th European Wireless Conference*, 2014, pp. 1–6.

[5] S. Monfared, T. Nguyen, L. Petrillo, P. De Doncker, and F. Horlin, "Experimental Demonstration of BLE Transmitter Positioning Based on AOA Estimation," in *In Proc. of the 29th IEEE Annual Intl. Symp. on Personal, Indoor and Mobile Radio Communications*, 2018, pp. 856–859.

[6] Z. Ma, S. Poslad, J. Bigham, X. Zhang, and L. Men, "A ble rssi ranking based indoor positioning system for generic smartphones," in *2017 Wireless Telecommunications Symposium (WTS)*, 2017, pp. 1–8.

[7] M. Cominelli, P. Patras, and F. Gringoli, "Dead on Arrival: An Empirical Study of the Bluetooth 5.1 Positioning System," in *Proc. of the 13th Intl. Workshop on Wireless Network Testbeds, Experimental Evaluation & Characterization*, 2019, pp. 13–20.

[8] Z. Hajiakhondi-Meybodi, M. Salimibeni, K. N. Plataniotis, and A. Mohammadi, "Bluetooth Low Energy-based Angle of Arrival Estimation via Switch Antenna Array for Indoor Localization," in *Proc. of the 23rd IEEE Intl. Conf. on Information Fusion*, 2020, pp. 1–6.

[9] M. Bresciani, R. Costanzi, V. Manzari, and D. Terracciano, "Acoustic tracking system for AUVs exploiting DoA sensors - calibration and performance characterisation," *IFAC-PapersOnLine*, vol. 52, no. 21, pp. 187–192, 2019, 12th IFAC Conference on Control Applications in Marine Systems, Robotics, and Vehicles.

[10] J. Traa, "Least-squares Intersection of Lines," University of Illinois Urbana-Champaign (UIUC), 2013.

[11] P. Abeles, "Efficent Java Matrix Library," 2020. [Online]. Available: https://ejml.org

[12] F. Pimenta, "Indoor Location based on AoA and Bluetooth Low Energy," Master's thesis, Faculdade de Engenharia da Universidade do Porto, Rua Dr. Roberto Frias S/N, Porto, Jul. 2020, TID: 202590267.

[13] R. E. Kalman, "A New Approach to Linear Filtering and Prediction Problems," *Transactions of the ASME–Journal of Basic Engineering*, vol. 82, no. Series D, pp. 35–45, 1960.

Authorized licensed use limited to: b-on: UNIVERSIDADE DO PORTO. Downloaded on May 05,2023 at 09:23:24 UTC from IEEE Xplore. Restrictions apply.